JOURNAL OF MATERIALS SCIENCE 33 (1998) 687–692

Elastic constants determination of thin cold-rolled stainless steels by dynamic elastic modulus measurements

SEUNG SEOK LEE, UN-SIG MIN, BONGYOUNG AHN
Failure Prevention Research Center, Korea Research Institute of Standards and Science, P.O. Box 102, Yu Song, Taejan 305-600, Korea
SEUNG HYUN YOO
Department of Mechanical Engineering, Ajou University, Suwon 442-749, Korea

Temperature dependence of elastic constants of thin cold-rolled stainless steel has been measured by using the acoustic resonance method. Identification of the vibration mode has been examined numerically and experimentally. The elastic constants at room temperature have also been measured by the pulse echo method. In addition, the texture effect on the elastic constants has been analysed by assuming the specimen has orthorhombic structure.

1. Introduction

Stainless steel has good corrosion resistance and mechanical properties at high temperature. The temperature dependences of elastic constants of the structural stainless steels are seldom found in the literatures [1–5] because those data are dependent on the processing variables such as composition or heat treatment. In this study, the temperature dependences of elastic constants of eight thin cold-rolled stainless steels were measured by the acoustic resonance method [6]. The range of Poisson's ratios at room temperature was found to be 0.16–0.45. Even though Poisson's ratio is very sensitive to the minor change of Young's modulus and shear modulus, the range of Poisson's ratio was considered too large. The pulse-echo method was employed for verification. The Poisson's ratio determined by the pulse-echo method was in the range 0.28–0.30, as expected [7]. Identification of the vibration mode and examination of the elastic anisotropic effect on the elastic constants were studied to determine the reasons.

2. Acoustic resonance method

2.1. Specimens

Eight cold-rolled stainless steels have been used for the measurements of the temperature dependence of elastic constants by the acoustic resonance method. The density and size of the specimens are shown in Table I.

2.2. Experiments and results

The dynamic elastic modulus of the specimens was measured using the resonance method [6] where the specimen was suspended by two carbon yarns as shown in Fig. 1. As the threads were attached to opposite sides of the specimen, both flexural and torsional resonant frequencies were obtained. The vibration was excited by a tweeter-type speaker that was connected to an HP 3324A synthesized function generator and detected by the phonograph cartridge. An SR-530 lock-in amplifier was used to amplify the weak pick-up signal. The resonant frequency at which the vibration amplitude showed a peak was determined by varying the frequencies. The experiment was carried out in vacuum. The shear modulus was then calculated according to the fundamental torsional resonant frequency using Equation 1 [6].

$$G = 4\rho RL^2 f_G^2 \quad (1)$$

where ρ is density, L is the length of the specimen, f_G is the torsional resonant frequency. R is a shape factor determined by the specimen geometry which can be found elsewhere [6]. The Young's modulus is calculated according to the fundamental flexural resonant frequency using Equation 2 [6].

$$E = 0.946\,42\left(\frac{L^2 f_E}{t}\right)^2 \rho T \quad (2)$$

TABLE I Geometry and density of the specimens

Material	Density ($g\,cm^{-3}$)	Thickness (mm)	Width (mm)	Length (mm)
STS304	7.899	1.195	14.96	70.05
STS304J1	7.897	0.784	14.95	70.04
STS304L	7.906	1.444	14.92	70.03
STS316	7.953	1.936	14.93	70.04
STS316L	7.955	0.751	14.94	70.03
STS410L	7.740	1.140	14.69	68.98
STS420J2	7.689	0.781	14.96	70.02
STS430	7.700	0.753	14.96	70.02

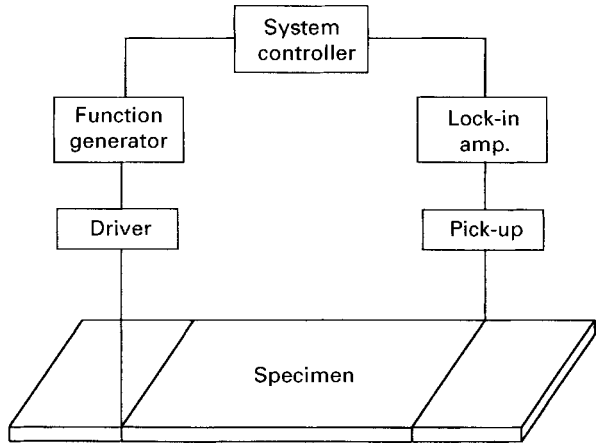

Figure 1 Geometry and density of the specimens.

where t is specimen thickness and T is the shape factor determined by the specimen geometry and the Poisson's ratio. The Poisson's ratio, σ, is obtained from the calculated Young's modulus and the shear modulus using the formula $\sigma = E/2G - 1$. The temperature dependence of elastic constants has been measured by putting the specimen inside the furnace. The elastic constants at high temperature are calculated from Equations 3 and 4

$$\frac{G(T)}{G(T_0)} = \left[\frac{f_G(T)}{f_G(T_0)}\right]^2 \frac{1}{1+\alpha\Delta T} \quad (3)$$

$$\frac{E(T)}{E(T_0)} = \left[\frac{f_E(T)}{f_E(T_0)}\right]^2 \frac{1}{1+\alpha\Delta T} \quad (4)$$

where $f_{G,E}(T)$ is resonant frequency at high temperature, and $f_{G,E}(T_0)$, $G(T_0)$, $E(T_0)$ are resonant frequency, shear modulus, Young's modulus at room temperature, respectively. α is thermal expansion coefficient, and ΔT is the temperature change.

The experimental results of elastic constants at room temperature are shown in Table II. 300 series stainless steels have the shear modulus of 72–76 GPa and a Young's modulus of 188–213 GPa. In 400 series stainless steels, the values of shear modulus are in the range of 84–89 GPa and the values of Young's modulus are in the range of 206–224 GPa. Poisson's ratios are in the range of 0.16–0.45. The range of the Poisson's ratios is considered very large even though the Poisson's ratio is very sensitive to the minor change of Young's modulus and shear modulus. Figs 2 and 3 show the temperature dependence of Young's modulus and shear modulus, respectively, up to 900 K. In the calculation, the value of $1.77 \times 10^{-5}\ K^{-1}$ was used as the thermal expansion coefficient for 300 series stainless steels and the value of $1.10 \times 10^{-5}\ K^{-1}$ was used for 400 series stainless steels. The temperature dependence of elastic constants was fitted with a linear form (a-bT) and a quadratic form (a-bT^2). Table III shows the values of the coefficients of determination when the temperature-dependent elastic constants were fitted with the above two forms. The results show that the elastic constants of 300 series stainless steels decrease linearly but those of 400 series stainless steels generally decrease in quadratic form as a function of temperature.

2.3. Numerical analysis

Equations 1 and 2, which calculate the elastic constants from the resonant frequencies, have been examined by numerical analysis. The resonant frequencies are calculated by the finite element method (FEM) using the Young's modulus and shear modulus obtained by the measured flexural resonant frequency and torsional resonance frequency as shown in Fig. 4. The general purpose FEM package ABAQUS has been used. In this figure, 1 means fundamental mode and 2 means the first overtone of the fundamental mode. The resonant data of 316L stainless steel were used in this calculation. The resonant values from numerical calculation do not show significant difference from the values from the resonant experiment. It means that the formulae are valid to the calculation of elastic constants from the resonant frequencies. However, there is a possibility of measuring the first overtone of flexural vibration instead of the fundamental torsional resonant frequency when they are close to each other.

TABLE II Shear modulus, Young's modulus, and Poisson's ratio of the specimens

Type	Ultrasonic method			Resonance method		
	G(GPa)	E(GPa)	σ	G(GPa)	E(GPa)	σ
304	77.2	200	0.295	75.5	208	0.381
$304J_1$	77.4	200	0.295	72.0	209	0.451
304L	77.3	200	0.294	74.3	205	0.381
316	76.5	198	0.294	76.1	213	0.398
316L	75.0	195	0.300	74.0	188	0.270
410L	82.9	213	0.286	84.3	224	0.329
$420J_2$	82.8	215	0.300	88.2	215	0.220
430	85.0	219	0.289	88.7	206	0.161
300 series[a]	75–77	195–200	0.294–0.300	72–76	188–213	0.270–0.451
400 series[b]	83–85	213–219	0.286–0.300	84–89	206–224	0.161–0.329

[a] Distribution of elastic constants of the above 300 series stainless steels.
[b] Distribution of elastic constants of the above 400 series stainless steels.

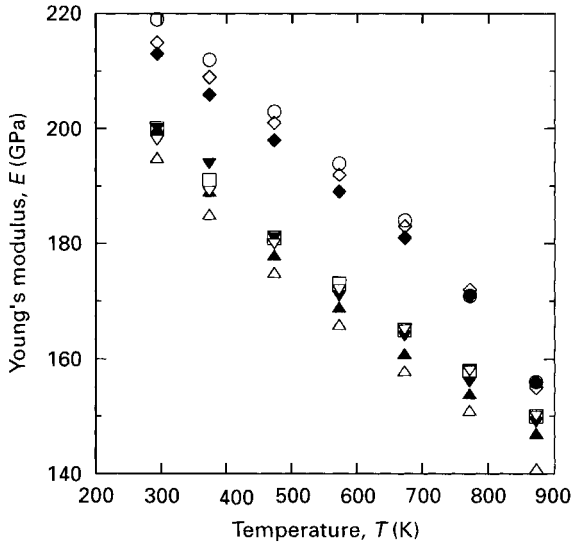

Figure 2 Temperature dependence of Young's modulus. (○) 430, (△) 316L, (◇) $420J_2$, (▼) $304J_1$, (◆) 410L, (▲) 304, (□) 304L, (▽) 316.

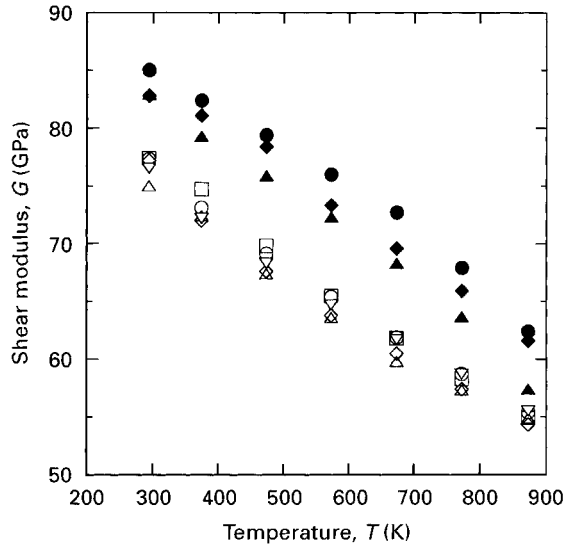

Figure 3 Temperature dependence of shear modulus. (●) 430, (△) 316L, (◆) $420J_2$, (□) $304J_1$, (▲) 410L, (◇) 304, (○) 304L, (▽) 316.

2.4. Identification of fundamental mode of torsional vibration

When a specimen vibrates in resonance, the type of vibration may be determined by probing. That is, the pick up is held slightly against different parts of the specimen while it is vibrating in resonance. If none of the settings of the equipment is altered during the course of probing, then the amplitude of the resonance peak is proportional to the mechanical vibrations of the portion of the specimen against which the probe is held. Fig. 5a shows the experimentally obtained probing amplitude at fundamental torsional resonant frequency in the 316L stainless steel, and (b) shows the vibration modes by ABAQUS in the specimen. There are nodes at the centre-lines and there are maximum amplitudes at the corners of the specimen in both (a) and (b). Therefore, the fundamental torsional vibration are measured correctly without confusion with the first overtone of the flexural vibration.

TABLE III The values of the coefficients of determination when the temperature-dependent elastic constants are fitted with linear form and quadratic form

	G		E	
	$a-bT$	$a-bT^2$	$a-bT$	$a-bT^2$
304	0.9840	0.9328	0.9852	0.9336
$304J_1$	0.9965	0.9634	0.9897	0.9469
304L	0.9943	0.9555	0.9942	0.9555
316	0.9910	0.9479	0.9944	0.9573
316L	0.9868	0.9390	0.9941	0.9584
410L	0.9901	0.9938	0.9887	0.9938
$420J_2$	0.9919	0.9893	0.9805	0.9968
430	0.9861	0.9974	0.9882	0.9975

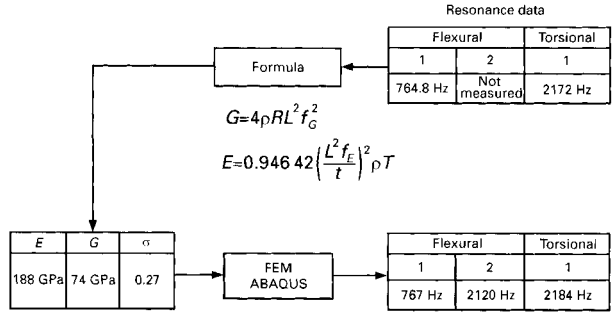

Figure 4 Resonant frequency examined by ABAQUS.

3. Pulse-echo method

A Pulser/Receiver (Panametrics, Model 5601A/TT) has been used for the generation and detection of ultrasonic waves. A digital oscilloscope (LeCroy, Model 9310) has been used for the measurement of time delay. The specimens were the same as those for the acoustic resonance method. The measurement direction was the through-thickness direction. The 20 and 10 MHz transducers were used for longitudinal and shear-wave velocity measurements, respectively. The polystyrene buffer rod was employed to overcome the overlapping of the main bang and the back echo signals. The shear modulus and the Young's modulus were calculated according to Equations 5a and b [8].

$$G = \rho V_s^2 \tag{5a}$$

$$E = \rho V_s^2 \frac{3V_l^2 - 4V_s^2}{V_l^2 - V_s^2} \tag{5b}$$

where V_s is the shear-wave velocity and V_l is the longitudinal wave velocity.

Significant anisotropy of shear-wave velocities was observed in the measurement of shear-wave velocities as shown in Table IV. The average value of fast and slow shear-wave velocities was used to calculate the elastic constants. The results are shown in Table II. The shear modulus and Young's modulus by the pulse-echo method are slightly different from those values from the resonant method. But the range of the Poisson's ratio by the pulse echo method is narrow compared with that by the resonant method. The Poisson's ratios determined by the pulse-echo method

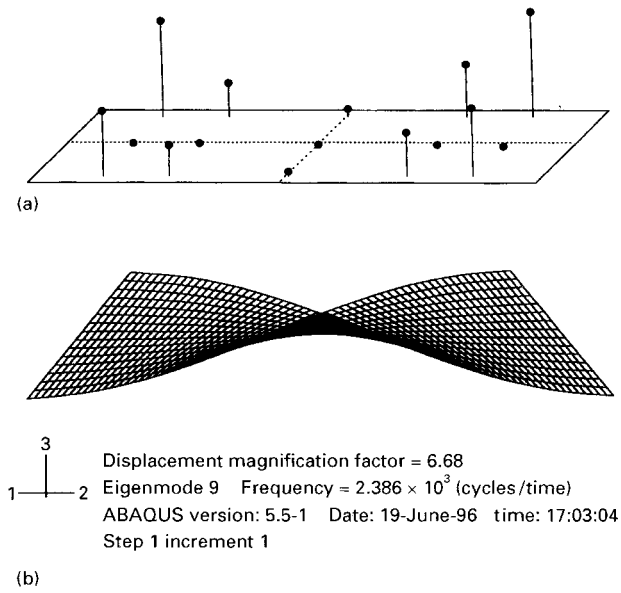

Figure 5 Torsional vibrational mode shape by (a) experimental measurements and (b) ABAQUS.

TABLE IV Two shear-wave velocities observed in the specimens

Specimen	Fast velocity (km s^{-1})	Slow velocity (km s^{-1})
304	3.148	3.140
304J$_1$	3.144	3.131
304L	3.166	3.098
316	3.290	2.917
316L	3.291	2.848
410L	3.352	3.206
420J$_2$	3.363	3.211
430	3.429	3.287

are in the range 0.28–0.3. However, the Poisson's ratios determined by the resonant method are in the range 0.16–0.45. It appears that averaging the two shear-wave velocities for the calculation of the elastic constants produces legitimate values of the Poisson's ratios.

4. Analysis of texture effect

It is assumed that the thin cold-rolled stainless steel has macroscopic orthorhombic symmetry [9, 10]. Let 0-xyz be the sample coordinate system with x, y, and z axes as the rolling, transverse, and normal directions. Following the Voigt procedure for averaging elastic constants of a polycrystal having a preferred orientation of the grains, Sayers [10] found that the nine polycrystalline elastic constants, C_{ij}, of an orthorhombic plate for the cubic crystallite might be expressed in terms of only six independent constants, W_{400}, W_{420}, and W_{440} (crystallite orientation distribution function, CODF coefficients [11–13]), and the single-crystal elastic constants, C_{11}^0, C_{12}^0 and C_{44}^0. The equations are written again in Equation 6a–i for completeness.

$$C_{11} = C_{11}^0 - 2C^0\left[\frac{1}{5} - \frac{6}{35}\sqrt{2\pi^2} \times\left(W_{400} - \frac{2}{3}\sqrt{10}W_{420} + \frac{1}{3}\sqrt{70}W_{440}\right)\right] \quad (6a)$$

$$C_{22} = C_{11}^0 - 2C^0\left[\frac{1}{5} - \frac{6}{35}\sqrt{2\pi^2} \times\left(W_{400} + \frac{2}{3}\sqrt{10}W_{420} + \frac{1}{3}\sqrt{70}W_{440}\right)\right] \quad (6b)$$

$$C_{33} = C_{11}^0 - 2C^0\left(\frac{1}{5} - \frac{16}{35}\sqrt{2\pi^2}\, W_{400}\right) \quad (6c)$$

$$C_{44} = C_{44}^0 + C^0\left[\frac{1}{5} - \frac{16}{35}\sqrt{2\pi^2}\left(W_{400} + \sqrt{\frac{5}{2}}W_{420}\right)\right] \quad (6d)$$

$$C_{55} = C_{44}^0 + C^0\left[\frac{1}{5} - \frac{16}{35}\sqrt{2\pi^2}\left(W_{400} - \sqrt{\frac{5}{2}}W_{420}\right)\right] \quad (6e)$$

$$C_{66} = C_{44}^0 + C^0\left[\frac{1}{5} + \frac{4}{35}\sqrt{2\pi^2}\left(W_{400} + \sqrt{70}W_{440}\right)\right] \quad (6f)$$

$$C_{31} = C_{12}^0 + C^0\left[\frac{1}{5} - \frac{16}{35}\sqrt{2\pi^2}\left(W_{400} - \sqrt{\frac{5}{2}}W_{420}\right)\right] \quad (6g)$$

$$C_{12} = C_{12}^0 + C^0\left[\frac{1}{5} + \frac{4}{35}\sqrt{2\pi^2}\left(W_{400} - \sqrt{70}\, W_{440}\right)\right] \quad (6h)$$

$$C_{23} = C_{12}^0 + C^0\left[\frac{1}{5} - \frac{16}{35}\sqrt{2\pi^2}\left(W_{400} + \sqrt{\frac{5}{2}}W_{420}\right)\right] \quad (6i)$$

where $C^0 = C_{11}^0 - C_{12}^0 - 2C_{44}^0$.

Kawashima [14, 15] gave the equations for the CODF coefficient W_{400}, W_{420}, and W_{440} from the relative ultrasonic velocity measurement using the Voigt approximation as shown in Equations 7a–c.

$$W_{400} = \frac{7}{16\sqrt{2\pi^2}}\left(\frac{5C_{44}^0 + C^0}{C^0}\right) \times\left[1 - \left(\frac{5C_{11}^0 + 10C_{44}^0}{2C^0 + 10C_{44}^0}\right)K_p\right] \quad (7a)$$

$$W_{420} = \frac{-7}{16\sqrt{2\pi^2}}\left(\frac{5C_{44}^0 + C^0}{C^0}\right) \times\left(\frac{5C_{11}^0 + 10C_{44}^0}{2C^0 + 10C_{44}^0}\right)K_m \quad (7b)$$

$$W_{440} = \frac{7}{8\sqrt{35\pi^2}}\left(\frac{5C_{44}^0 + C^0}{C^0} + \frac{4\sqrt{2\pi^2}W_{400}}{7}\right) \times\left(1 - \frac{1}{K_3}\right) \quad (7c)$$

TABLE V The comparison of isotropic and anisotropic analysis by the resonant frequencies

	Experimental (Hz)	Isotropic			Anisotropic		
		E, G	ABAQUS →	Resonant frequencies (Hz)	C_{ij}	ABAQUS →	Resonant frequencies (Hz)
Flexural	765			781			787
Torsional	2172			2199			2174

Here, the details of K_p, K_m, and K_3 can be obtained from Kawashima [14]. Following Kawashima [14, 15], W_{400} and W_{420} were obtained from the ratio of the resonance frequencies of slow shear waves, fast shear waves and longitudinal waves measured by the thickness resonance method. W_{440} was obtained from measurements of the velocities of the fundamental horizontally polarized shear mode (SH_0) propagated at 0° and 45° from the rolling direction in the plane of the plate.

316L stainless steel has been used for the analysis of texture effect because the specimen has the maximum anisotropy. The specimen is the square type plate of 200 mm × 200 mm × 0.751 mm. To measure the resonance frequencies of the through-thickness modes, an EMAT [14] was made using a spiral coil of 30 mm diameter and a disc-type Nd-Fe-B permanent magnet of 20 mm diameter. This EMAT generates and receives the longitudinal and shear waves simultaneously. The measurement was performed with a superheterodyne phase sensitive detector system (RAM 10000, Ritec, Inc.) [16]. The measured resonant frequencies were ranged in 0.5–5 MHz. The burst width for exciting the transmitter and the integrator gate width were 40 and 100 μs, respectively. The detailed principles of resonant frequency measurement are described elsewhere [14–16]. A different kind of EMAT [16] was also made to measure the transit time of the horizontally polarized shear wave (SH wave) propagated along the tangential direction of the plate surface. This EMAT consists of 48 magnets of $2.4 \times 5\ mm^2$ and an elongated spiral coil. It was excited by the tone burst pulse of 660 kHz. The distance between the transmitter and receiver was about 120 mm. From the above measurement, three CODF coefficients were obtained, $W_{400} = 4.39 \times 10^{-3}$, $W_{420} = -5.76 \times 10^{-3}$, and $W_{440} = -8.46 \times 10^{-4}$. For the calculation of those coefficients, the single-crystal elastic constants of 316 stainless steel ($C^0_{11} = 206$ GPa, $C^0_{12} = 133$ GPa, $C^0_{44} = 119$ GPa [18]) were used because the single-crystal elastic constants of 316L stainless steel were not available in the literature. The present ultrasonic method is affected by the chosen values of the single-crystal elastic constants used in the calculation. Therefore, directly measurable elastic constants from the above experiment, such as $C_{33}, C_{44}, C_{55}, C_{66}$ were taken instead of the calculated elastic constants from CODF coefficients and the single-crystal elastic constants. The following nine elastic constants were obtained from the above analysis.

$C_{11} = 261$ GPa $C_{22} = 280$ GPa $C_{33} = 263$ GPa

$C_{44} = 63$ GPa $C_{55} = 82$ GPa $C_{66} = 85$ GPa

$C_{23} = 83$ GPa $C_{31} = 104$ GPa $C_{12} = 99$ GPa

Table V shows the comparison of isotropic and anisotropic analysis by the resonant frequencies. Isotropic analysis means that the resonant frequencies are numerically calculated from two elastic constants which were obtained from the pulse-echo method. Anisotropic analysis means that the resonant frequencies are numerically calculated from the above nine elastic constants. From the anisotropic analysis, the calculated torsional resonant frequency is very close to the experimental value because the relevant elastic constants for the calculation of torsional vibration are directly measured ultrasonic data. The discrepancy still exists in the flexural resonant frequency because of the inaccurate single-crystal elastic constants.

5. Conclusion

From the acoustic resonance method, the austenitic stainless steels (300 series) are shown to have a Young's modulus of 188–213 GPa and a shear modulus of 72–76 GPa at room temperature. Ferritic and martensitic stainless steels (400 series) have a Young's modulus of 206–224 GPa and a shear modulus of 84–89 GPa. The temperature dependence of elastic constants of 300 series stainless steel decreases linearly, but that of 400 series stainless steel decreases in quadratic form. Finally, the reason for the large range of Poisson's ratio determined by the acoustic resonance method is shown to be due to the anisotropy of the materials.

Acknowledgement

We are indebted to Dr Yun Young Lee Pohang Steel Company, for providing all the samples.

References

1. R. F. S. HEARMON, "Landolt-Börnstein, Numerical Data and Functional Relationships in Science and Technology" (Springer, Berlin, 1979).
2. J. P. HAMMOND, L. T. RATCLIFF, C. R. BRINKMAN, M. W. MOYER and C. W. NESTER Jr, "Dynamic and Static Measurements of Elastic Constants with Data on 2 1/4 Cr-1 Mo Steel, Types 304 and 316 Stainless Steels, and Alloy 800H", ORNL-5442 (Oak Ridge National Laboratory, Oak Ridge, TN, 1979).
3. J. P. HAMMOND and C. R. BRINKMAN, "Heat-to-Heat and Directionality Variations of Elastic Constants in Types 304 and 316 Stainless Steel and 2 1/4 Cr-1 Mo Steel", ORNL/TM-6879 (Oak Ridge National Laboratory, Oak Ridge, TN, 1979).

4. H. M. LEDBETTER, N. V. FREDERICK and M. W. AUSTIN, *J. Appl. Phys.* **51** (1980) 305.
5. H. M. LEDBETTER, *ibid.* **52** (1981) 1587.
6. S. SPINNER and W. E. TEFFT, *ASTM Proc.* **61** (1961) 1221.
7. W. KÖSTER and H. FRANZ, *Metall. Rev.* **6** (1961) 1.
8. E. SCHREIBER, O. L. ANDERSON and N. SOGA, "Elastic Constants and Their Measurement" (McGraw-Hill, New York, 1973).
9. R. B. THOMPSON, S. S. LEE and J. F. SMITH, *J. Acous. Soc. Am.* **80** (1987) 921.
10. C. M. SAYERS, *J. Phys. D Appl. Phys.* **15** (1982) 2157.
11. R.-J. ROE, *J. Appl. Phys.* **36** (1965) 2024.
12. *Idem., ibid.* **37** (1966) 2069.
13. H. J. BUNGE, *Kristall Technik* **3** (1968) 431.
14. K. KAWASHIMA, *J. Acous. Soc. Am.* **87** (1990) 681.
15. K. KAWASHIMA, T. HYOGUCHI and T. AKAGI, *J. Nondes. Eval.* **12** (1993) 71.
16. H. FUKUOKA, M. HIRAO, T. YAMASAKI, H. OGI, G. L. PETERSON and C. M. FORTUNKO, in "Review of Progress in QNDE", Vol. 12, edited by D. O. Thompson and D. E. Chimenti (Plenum, New York, 1993) p. 2129.
17. C. F. VASILE and R. B. THOMPSON, *J. Appl. Phys.* **50** (1979) 2583.
18. H. M. LEDBETTER, *Br. J. NDT* (1981) 286.

Received 17 September 1996
and accepted 22 August 1997